Cytometric analysis of immune cell populations in clinical tumor biopsy tissue microarrays for immuno-oncology

Patel, J.[1], Krisanits, B.[1], Collins, K.[2], Lillard, K.[2], Villani, T.S.[1]
[1]Visikol Inc., Shelbourne Bldg, 53 Frontage Rd., Hampton, NJ
[2]Indica Labs, Albuquerque, NM

VISIKOL A BICO COMPANY

indica labs QUANTITATIVE PATHOLOGY

Introduction

Cancer is a deadly complex disease that affects millions around the world each year. Variability in disease etiology leads to challenges in selecting treatments that will maximize the patient's quality of life and overall survival. It is essential for health care providers to know the extent of a patient's cancer to better prescribe a treatment to improve prognosis. However, current methods of patient diagnosis are qualitative and/or semi-quantitative and may not include the impact of the tumor micro-environment on patient treatment and outcome. Therefore, we have developed a method utilizing 12-plex fluorescence imaging, quantitative image analysis, as well as cytometric analysis of immune cell populations to better categorize patients and determine the best treatment strategy for the individual patient.

"[T]here is considerable heterogeneity within each TME category, adding uncertainty to the reproducibility of the current classification of "cold" vs. "hot" vs. "intermediate" immune-subtypes."
- Bairi et al., Nature Breast Cancer (2021) 7:150;

Workflow

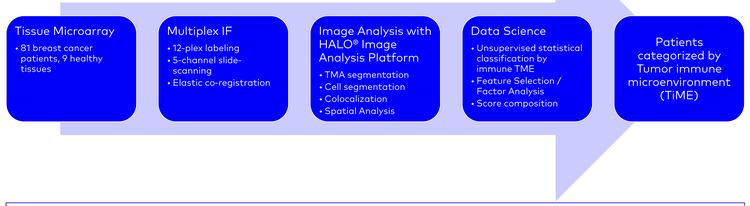

Materials and Methods

Multiplex labeling was completed on human breast cancer tissue microarray (TMA) (XBra089-01) using traditional immunofluorescence labeling techniques. The TMA was rehydrated through decreasing ethanol concentrations, followed by antigen retrieval in citrate buffer. Labeling of the TMA was completed in 4 panels with a control nuclear stain DAPI, designed to reduce cross-reactivity and promote labeling sensitivity. Removal of antibody labeling between panels was completed using Visikol Inc's proprietary stripping reagent EasyPlex™. Imaging was completed at 40x on the Leica Versa 8 slide scanner.

Once the fluorescence imaging was complete, HALO v3.3 was used for the analysis by first using the HALO TMA module to tile the cores into individual image sets. The individual cores were analyzed using the HALO Highplex module v4.0.4, to perform cell segmentation and marker colocalization. Subsequently, the HALO Spatial Analysis module was utilized to perform a proximity analysis between different cell subtypes. After exporting this data from HALO as a .csv file, well-established python libraries (Pandas, SciPy, and Scikit-Learn), were used to analyze the data.

Quantitative measurement data were normalized and standardized using the standard scaling technique resulting in mean-centered values representing the number of standard deviations from the mean. To select a subset of features based on their contribution to the variation between groups, feature selection was performed using the F-test. To visualize patient population-wide variation and clustering from the selected feature subsets, principal component analysis (PCA) was conducted. Clustering of samples and measurements was conducted using hierarchical agglomerative clustering of the Euclidean distance matrix from selected feature subsets.

Cohort Population Overview

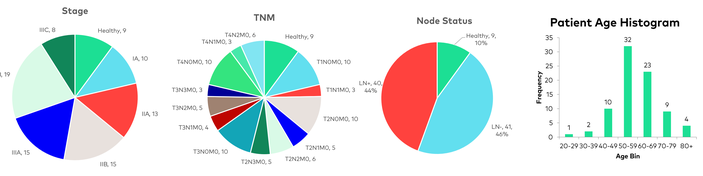

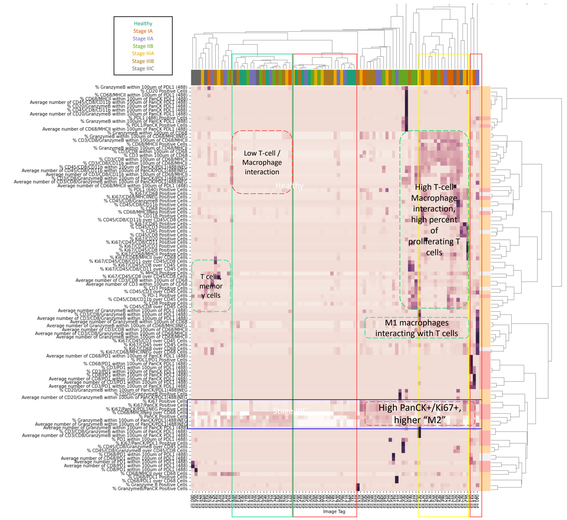

Figure 1: Clustered Heatmap of patients (color coded along top x-axis by stage, see legend) for all measured immunophenotypical features measured in the cohort. As indicated, several clear subcategories emerge, representing a spectrum from highly active immune response (green dashed outlines) and immunosuppressive response (red dashed outlines)

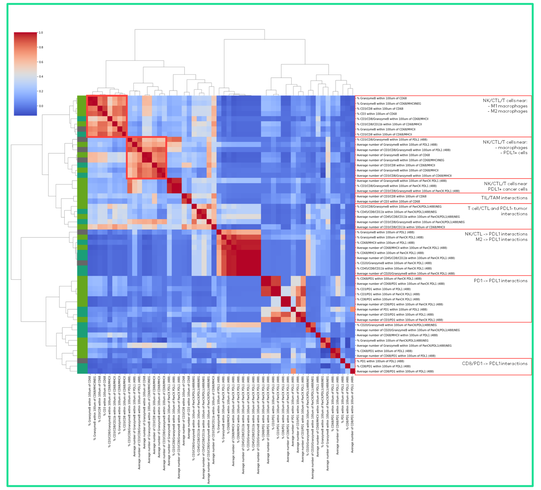

Figure 2: Correlogram depicting correlational trends between interacting subtypes of immune cells within the tumor immune microenvironment measured within the cohort. Several distinct relationships were detected, highlighted in red outlines on the figure.

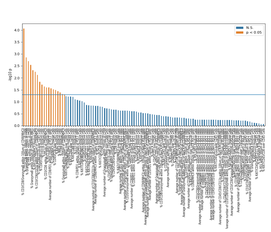

Figure 3A: Rank-order of feature-importance measured via the F-test illustrating features most significant to accounting for differences between stages of patients within the cohort.

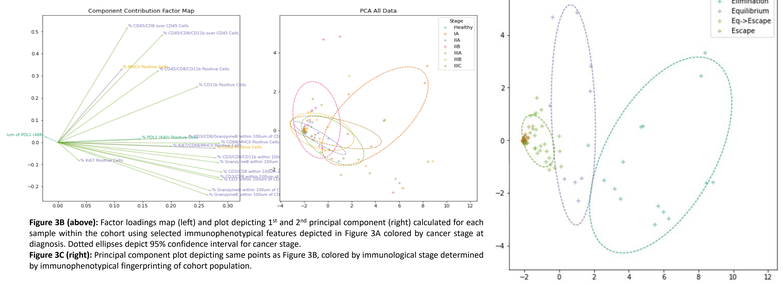

Figure 3B (above): Factor loadings map (left) and plot depicting 1st and 2nd principal component (right) calculated for each sample within the cohort using selected immunophenotypical features depicted in Figure 3A colored by cancer stage at diagnosis. Dotted ellipses depict 95% confidence interval for cancer stage.
Figure 3C (right): Principal component plot depicting same points as Figure 3B, colored by immunological stage determined by immunophenotypical fingerprinting of cohort population.

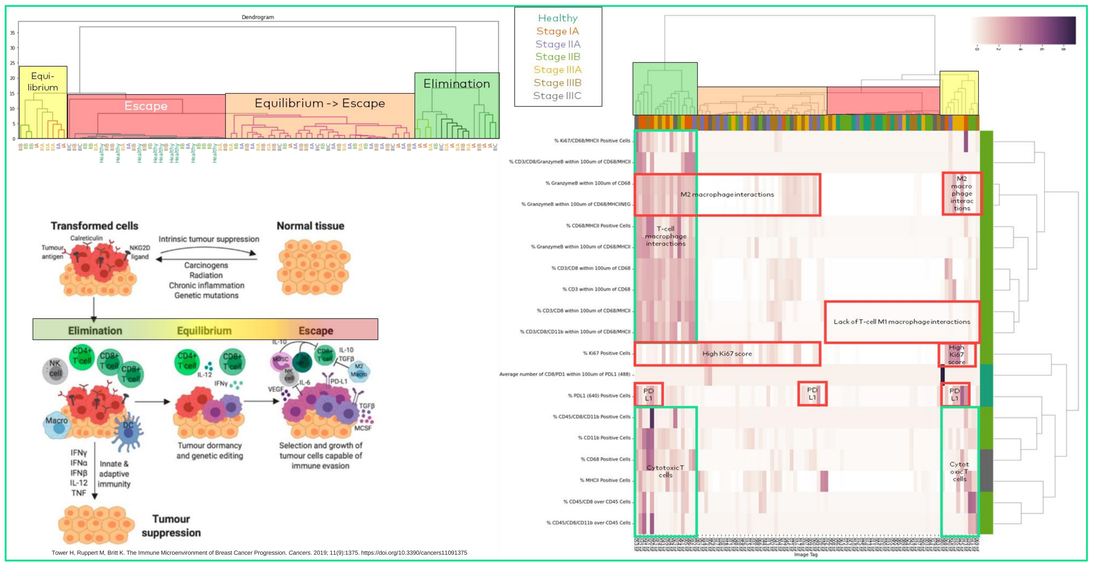

Tower H, Ruppert M, Britt K. The Immune Microenvironment of Breast Cancer Progression. *Cancers*. 2019; 11(9):1375. https://doi.org/10.3390/cancers11091375

Figure 4: An illustration of the immune microenvironment response within the tumor (bottom left), which shows how tumor cells are eliminated at first by immune cells, then go into equilibrium with the immune system, and finally escape the immune system altogether. The dendrogram (top left) shows how the patients fit this pattern, and the clustered heatmap (right) further shows this by highlighting features prevalent at each of the stages in the immune microenvironment response.

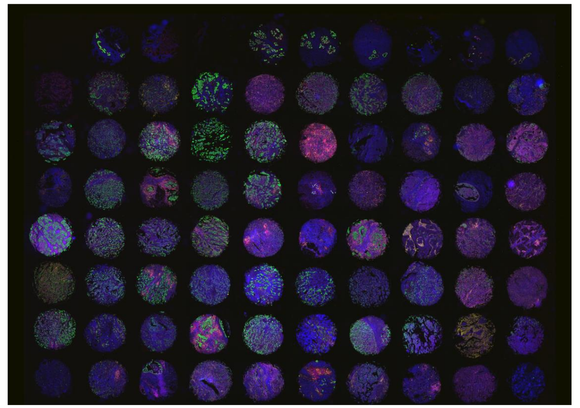

Results and Discussion

Intercommunication between immune cells and the tumor microenvironment (TME) is a dynamic process that consists of complex feedback between immunosurveillance and tumor progression, known as immunoediting. Immunoediting progresses to impact aspects of tumor biology in three distinct phases: elimination, equilibrium, and escape. During the "elimination phase," the TME consists of innate and adaptive immune responses to tumor cells, which in earlier stages contribute to the elimination of tumor cells. However, adaptive pressure upon the tumor cells which survive causes shifts in the phenotype of the tumor cells towards the "equilibrium phase"—during which the TME transitions towards a non-immunogenic phenotype, promoting tumor progression. Cells that survive by acquired resistance to elimination enter the "escape phase", promoting cancer cell growth and expansion in an uncontrolled manner. At this stage, the tumor immunophenotype is non-immunogenic, very few immune cells are detected, and the tissue resembles healthy tissue from an immunological perspective.

Utilizing 12-plex fluorescence imaging of TMA, quantitative image analysis, as well as cytometric analysis of immune cell populations we showed discrete subpopulations of breast cancer patients exhibiting immunological signatures across the transitional phases of immunoediting (Figure 1). Several distinctive immunological phenotypes were observed, ranging from highly inflamed patients with significant T-cell-macrophage interactions, to a large number of patients with immunological phenotypes indistinguishable from healthy patients (see groupings in Figure 1). To better understand correlations between cell-cell interactions within the TME, a correlogram was generated, and as indicated on Figure 2, there was a high degree of correlation between the coincidence of interactions between macrophages and various T-cells/NK-cell subtypes, and proximity to immune checkpoint inhibitor PD-L1, promoting the treatment of this subgroup of patients with immune checkpoint inhibitors such as PD-L1 inhibitors.

Using statistical techniques, the most significant measurements (i.e. "features") of differences in immunological phenotype between patients in different stages of cancer progression were ranked using the F-test (Figure 3A) and selecting measurements based on a p-value threshold. The resulting subset of measurements (highlighted in orange on Figure 3A). was used for subsequent analyses. To visualize the contributions of the features to the population-wide variation among patients, principal component analysis (PCA) was conducted, selecting the first and second component for plotting on the x and y axis, respectively. The factor-loadings map, shown in the left panel of Figure 3B, illustrates the contributions of each measurement to the variation across the population. The PCA plot shown in the right-side panel of Figure 3B is colored by the patient's stage, with confidence ellipses around the patients in each stage, illustrating significant heterogeneity of immunophenotype within each stage, as seen by the high degree of overlap between the stages on the plot. Figure 3C depicts the same plot as Figure 3B, however the plot is colored by the proposed phase of immunoediting which the phenotype corresponds to, as determined by the clustering analysis described in Figure 4. Figure 3C illustrates the clear delineation of the transition from the "elimination" phase to the "escape" phase. The proper determination of the immunophenotype corresponding to each phase of the immunoediting transition is critical to personalized medicine and to properly identify suitable therapeutic treatments for a given patient.